

## Optimized ammonium removal using Al-modified bentonite: Insights into structural and mineralogical changes

Thao Hoang-Minh<sup>1\*</sup>, Lan Nguyen-Thanh<sup>2</sup>, Nga Thi Pham<sup>3</sup>, Dong Van Bui<sup>1</sup>, Nguyen Thi Hai<sup>1</sup>, Thai Dinh Nguyen<sup>1</sup>, Thuyet Minh Thi Nguyen<sup>1</sup>, Thien Duy Nguyen<sup>1</sup>, Rafael Ferreira Mählmann<sup>2</sup>, Jörn Kasbohm<sup>4</sup>

<sup>1</sup>University of Science, Vietnam National University, Hanoi, Hanoi, Vietnam

<sup>2</sup>Institute of Applied Geosciences, Technical University Darmstadt, Schnittspahn Str. 9, 64287 Darmstadt, Germany

<sup>3</sup>Graduate School of Creative Sciences and Engineering, Waseda University, 3-4-1 Ookubo, Shinjuku, Tokyo, Japan

<sup>4</sup>Jörn-Kasbohm-Consulting and Greifswald University, 17487 Greifswald, Germany

Received 17 December 2024; Received in revised form 20 February 2025; Accepted 28 February 2025

### ABSTRACT

Highly effective adsorbents derived from modified Di Linh bentonite (Lam Dong Province, Vietnam) were produced using  $\text{Al}^{3+}$  stock solution prepared from  $\text{Al}_2(\text{SO}_4)_3 \cdot 18\text{H}_2\text{O}$ . Mineral, morphology, and surface area properties of untreated and Al-modified Di Linh bentonite were characterized using X-ray diffraction, Fourier transform infrared spectroscopy, scanning electron microscopy, and nitrogen adsorption-desorption analyses. A scanning experiment was conducted to investigate the Al-modified bentonite material's ammonium ( $\text{NH}_4^+$ ) removal capacity at two levels of  $\text{NH}_4^+$  initial concentration. Results show that the combination of acid  $\text{H}_2\text{SO}_4$  (a bioproduct of diluted Al solution) with  $\text{Al}^{3+}$  caused the smectitization of clay particles via a dissolution-precipitation mechanism, which enhances the structural organization of smectite and modifies its mineralogical properties. This process promoted the removal capacity of Al-modified bentonites, which increased to 0.47 mg/g in comparison with 0.32 mg/g from untreated bentonite at 50 mg/L  $\text{NH}_4^+$ -N concentration, to 19.3 mg/g in comparison with 17.2 mg/g from untreated bentonite at 1000 mg/L  $\text{NH}_4^+$ -N concentration. This approach to modifying natural bentonite offers new possibilities for developing adsorbents to eliminate  $\text{NH}_4^+$  from water.

*Keywords:* Al-modified bentonite, ammonium removal, adsorption property, clay, smectitization.

### 1. Introduction

Ammonium ( $\text{NH}_4^+$ ) is the inorganic ion form of N that can result from the decomposition of organic nitrogen compounds found in domestic and industrial wastewater, municipal sewage, and water (Han et al., 2021). Ammonium can lead to eutrophication,

resulting in the depletion of dissolved oxygen, toxicity to the aquaculture system, and decreased species diversity (Edwards et al., 2023). The World Health Organization (WHO) states that  $\text{NH}_4^+$  can be toxic or dangerous to health if its concentration in the human body exceeds 200 mg/kg of body weight (WHO, 2011). The WHO reported that excess  $\text{NH}_4^+$  in water can diminish disinfection efficiency, lead to nitrite

\*Corresponding author, Email: [hoangminhthao@vnu.edu.vn](mailto:hoangminhthao@vnu.edu.vn)

formation in the water system, create odor in water, and impair manganese removal. Nitrite levels should be maintained below 0.1 mg/L to prevent potential toxicity, while total transformation of 1 g ammonium results in 2.7 g nitrite.

In recent years, many kinds of techniques for the removal of ammonium from water have been widely studied, including air stripping (Sotoft et al., 2015), biological treatment processes (Abu Hasan et al., 2013), chemical precipitation (Chai et al., 2017), anammox (Yang et al., 2019), photoelectrocatalytic (Ji et al., 2017), and adsorption (Tu et al., 2019; Cheng et al., 2019) methods. Biological treatment is the principal and effective method for accessing domestic wastewater treatment plants. This technique is considered the most economical method for ammonium/ammonia treatment at wastewater treatment plants (Liu et al., 2019). However, when water or environmental conditions, including temperature, change, the growth rate of microorganisms and the biological activities of the biological treatment system will be affected (dos Santos and Daniel, 2020). Adsorption and/or ion exchange are widely regarded as the most viable methods for eliminating ammonium from water because they are more direct, stable, and inexpensive methods. Therefore, it is possible to develop adsorbents and/or ion-exchangeable materials for removing ammonium before or after biological treatment (Cheng et al., 2019). Consequently, there has been a global interest in developing cost-effective and efficient natural materials for removing ammonium in water treatment (Cheng et al., 2019; Lin et al., 2014; Tran et al., 2022;). Numerous studies on ammonium removal have concentrated on clay materials (Angar et al., 2017; Zamparas et al., 2013).

From ancient to modern times, clay materials have been utilized in various applications, such as building materials,

earthenware, ceramic products, paper, rubber, paint, pharmaceuticals, cosmetics, and adsorbents. The application of specific clay materials is based on the primary clay minerals and their physical and chemical properties, which are strongly influenced by the structure and composition of the clay minerals (Murray, 2007). Clays play an essential role in the environment by serving as natural scavengers of pollutants, absorbing both anions and cations through adsorption or ion exchange processes. These materials excel as adsorbents due to various active sites on their surfaces, including Bronsted and Lewis acid sites and ion exchange sites. Ammonia undergoes protonation by acidic water molecules at the interface of exchangeable cations (Rybalkina et al., 2019). Subsequently, ammonium comes into contact with exchangeable cations and participates in the cation exchange reaction with clay. Among clay families, bentonite and bentonitic clay are the best adsorbents because of their main clay mineral's high surface charge, high ion exchange capacity, and very high specific surface area, smectite (Murray, 2007).

Numerous researchers have employed bentonite to remove various hazardous substances, including ammonium, from water and wastewater (Anggraini et al., 2014; Campos et al., 2013; Cheng et al., 2019; Yao et al., 2014). Otherwise, the negative charge of clay minerals in general and bentonite, in particular, can be repelled by natural clay minerals, which is a reason for the ineffective adsorption of these contaminants. When examining the elimination of biological, organic, and inorganic contaminants from drinking water, Srinivasan asserted that clays and their modified composites demonstrate either superior or comparable adsorption capacities for pollutants compared to other inexpensive adsorbents (Srinivasan, 2011). Many prior studies on ammonium adsorption have also concentrated on clay materials

(Zamparas et al., 2013). However, bentonite and bentonitic clay are composed of tiny swelling particles of montmorillonite, illite/smectite mixed-layer (IS-ml), and dioctahedral vermiculite/smectite mixed-layer (diVS-ml) minerals. Both of these properties prevent water migration through bentonite and bentonitic clay. Using natural bentonite in fixed-bed adsorption for water or wastewater treatment systems is challenging or impractical. Hence, modification is necessary to convert bentonite or bentonitic clay into an effective material for ammonium removal.

There has been a notable focus on the combination of bentonite with various materials, including metals, synthetic polymers, and natural polymers (Dukic et al., 2015; Ianchis et al., 2015; Pandey, 2017; Rzaev et al., 2015; Srinivasan, 2011; Vanamudan and Pamidimukkala, 2015). Clays modified with metals are highly significant due to their high thermal stability, extensive surface area, and inherent catalytic activity (Angar et al., 2017). Sun et al. (2015) used purified low-grade natural Ca-bentonite and modified it with  $\text{Na}^+/\text{Al}^+$ . The authors found that the ammonium adsorption capacity of purified and modified bentonite was nearly twice that of raw bentonite, which was among the highest values of ammonium adsorption (46.90 mg/g) compared with many popular adsorbents, including natural zeolite and synthesized zeolite from fly ash. The modification process, however, depends on various other factors, including pH, temperature, duration, and the ratio of materials. In a consecutive study, Cheng et al. (2019) modified bentonite with  $\text{Al}^{3+}$  cross-linked with tannin to form a promising adsorbent to remove ammonium from wastewater at room temperature. Modifying clays through pillaring and activation significantly impacts their structural properties, often enhancing their adsorption capacities. However, reverse trends are also observed in some cases.

This study used raw Di Linh bentonite from Lam Dong Province, Vietnam, as the starting material. The bentonite was modified using  $\text{Al}_2(\text{SO}_4)_3 \cdot 18\text{H}_2\text{O}$  solutions at various concentrations to assess its effectiveness in removing ammonium from aqueous solution. The objective was to explore the structural and mineralogical changes during the modification process. Different analytical techniques were applied in the study, including X-ray diffraction (XRD), Fourier transform infrared spectroscopy (FT-IR), scanning electron microscopy (SEM), and adsorption-desorption of  $\text{N}_2$  at 77 Kelvin, to characterize the solid materials in the samples.

## 2. Materials and Methods

### 2.1. Materials

The natural bentonite is of sedimentary origin and is located in the bentonite-, diatomite- and lignite-bearing Di Linh Formation in Lam Dong Province, Southern Vietnam. This clay/bentonite has been regarded as a lacustrine sediment that is locally stratiform and interbedded with some basalt. Hoang-Minh et al. (2019) investigated and published this clay's chemical composition and crystallinity, especially for the  $<2.0 \mu\text{m}$  fraction. This clay was used after removing coarse fractions of nonclay-sized impurities by sieving and sedimentation. The aluminum sulfate hydrate ( $\text{Al}_2(\text{SO}_4)_3 \cdot 18\text{H}_2\text{O}$ ) and  $\text{NH}_4\text{Cl}$  were purchased as analytical grade reagents from Sigma-Aldrich as an Al-source and ammonium without further purification.

### 2.2. Preparation of Al-modified bentonites

The natural Di Linh bentonite was gently hand-milled in an agate mortar to a fine powder, and the  $<40 \mu\text{m}$  fraction was separated by sieving. The  $\text{Al}^{3+}$  stock solution was prepared by diluting  $\text{Al}_2(\text{SO}_4)_3 \cdot 18\text{H}_2\text{O}$  to different concentrations (0 ppm, 5 ppm, 50 ppm, 100 ppm, 150 ppm, 250 ppm, and 500 ppm), which are designated as C1.1, C1.2, C1.3, C1.4, C1.5, C1.6, and C1.7,

respectively. The prepared stock solutions were saturated with natural Di Linh bentonite with a solid: liquid ratio of 1:10. The mixture of clay and  $\text{Al}^{3+}$  stock was agitated for 180 minutes at 80 rpm using a reciprocating shaker, after which the mixture was centrifuged for 60 minutes at 400 rpm to separate the liquid and solid parts. The supernatants were subsequently filtered through a  $0.25 \mu\text{m}$  filter for further measurements. The solid material was dried and milled again by agate mortar to a fine powder. A portion of the sample was chemically and physicogenically investigated via XRD, FT-IR, SEM, CEC, and BET-specific surface analysis, and the other parts were used for  $\text{NH}_4^+$ -adsorption experiments.

### 2.3. Mineralogical characterization

XRD determined semiquantitative mineral composition and structural properties of each phase. The XRD patterns were obtained from bulk samples (randomly oriented powders) and clay fraction ( $<2.0 \mu\text{m}$ )-oriented mounts (both air-dried and ethylene-glycolated specimens). The XRD measurements were performed using a Panalytical X'Pert Pro Diffractometer. The equipment was operated at 30 mA and 40 kV, employing  $\text{Cu-K}\alpha_{1,2}$  radiations and a step size of  $0.008^\circ 2\theta$ . The data were collected within the range of  $4$  to  $70^\circ 2\theta$  for bulk samples and  $4$  to  $35^\circ 2\theta$  for oriented mounts.

FT-IR also was performed at room temperature, spanning from  $400$ - $4000 \text{ cm}^{-1}$  with a resolution of  $4 \text{ cm}^{-1}$  to characterize mineralogical composition. Powder samples (1 to 2 mg) were uniformly mixed with 120 mg of predried KBr (at  $80^\circ\text{C}$ ) for a minimum of 6 hours. Pellets of the mixture with a diameter of 13 mm were formed and inserted into the Varian 670-IR series for analysis. Origin Pro 2021 Peak Fitting with Gaussian distribution was used to deconvolute the yielded FT-IR spectra. The obtained bands were compared with the values Farmer (1974)

and Madejová & Komadel (2001) reported to determine the mineral structure.

### 2.4. Morphology and surface area characterization

SEM images were obtained on hand-powdered natural and modified Di Linh clays to characterize the morphology of the clay materials. This method used FEI Quanta 400 ESEM FEG equipment and an energy-dispersive X-ray system (Oxford, Oxfordshire, UK).

The BET-specific surface area of representative samples (C1.1, C1.4, and C1.6) was employed using a Quantachrome NOVA 2000e series volumetric gas adsorption instrument. The materials were degassed under vacuum, weighed, and cooled using external liquid nitrogen. The nitrogen gas pressure gradually increases from vacuum to  $0.995 \text{ atm}$ , causing physico-sorption on the clay surface, and an adsorption isotherm is recorded. The nitrogen pressure is subsequently decreased back to the vacuum, and a desorption isotherm is documented. The specific surface area, pore volume, size distribution, and  $\text{N}_2$  adsorption-desorption isotherms at  $77 \text{ Kelvin}$  were archived.

The exchangeable cations were determined using  $0.1 \text{ M BaCl}_2$ , and the cation exchange capacity (CEC) was calculated as the sum of the exchangeable  $\text{Ca}^{2+}$ ,  $\text{K}^+$ ,  $\text{Na}^+$ , and  $\text{Mg}^{2+}$  ions.

### 2.5. Ammonium adsorption experiments

The adsorption of ammonium from the  $\text{NH}_4\text{Cl}$  solution by participants in the Al-modified bentonite was conducted in a batch process at room temperature. Ammonium solutions with initial concentrations of  $50 \text{ mg/L}$  and  $1000 \text{ mg/L}$  were created by adding the necessary amount of  $\text{NH}_4\text{Cl}$  to reverse osmosis-grade water. In a series of  $100 \text{ mL}$  flasks containing  $50 \text{ mL}$  of solution,  $0.5 \text{ g}$  of Al-modified bentonite (adsorbent) was added ( $10 \text{ g/L}$  adsorbent concentration).



The flasks were subsequently shaken at 100 rpm for 6 h. After reaching equilibrium, the solution was separated from the adsorbents by centrifugation at 3000 rpm for 10 minutes. The initial and equilibrium concentrations of ammonium were assessed through static headspace gas chromatography utilizing an Agilent 6890 GC.

The  $\text{NH}_4^+$  adsorption capacities (mg/g) at the equilibrium ( $q_e$ ) were determined by the following equation:

$$q_e = \frac{(C_o - C_e)V}{m}$$

where  $C_o$  (mg/L) and  $C_e$  (mg/L) are the  $\text{NH}_4^+$  concentrations at initial and equilibrium, respectively;  $m$  (g) is the adsorbent mass;  $V$  (L) is the solution volume.

### 3. Results and Discussions

#### 3.1 Mineral characterization

The XRD profiles and quantification of the mineralogical composition of the unmodified and modified samples are shown in Fig. 1 and Table 1. The untreated and treated Di Linh bentonites are composed mainly of montmorillonite and consist of mica (illite + muscovite), kaolinite as a clay mineral and quartz, and feldspars (microcline) as impurities. Smectite samples exhibited a d-spacing reflection of  $d(001) = 15.3 \text{ \AA}$  for natural Di Linh smectite, indicating the presence of divalent cations ( $\text{Ca}^{2+}$  and  $\text{Mg}^{2+}$ ) in the interlayer sheet of montmorillonite, and  $d(001) = 14.4\text{--}14.9 \text{ \AA}$  for Al-modified smectites, suggesting a higher presence of monovalent cations ( $\text{Na}^+$ ) of montmorillonite. Montmorillonite also exhibited nonbasal reflections with  $d \approx 4.47, 2.56, 1.68 \text{ \AA}$  and other small nonbasal reflection values. Reflections of  $d(060)$  at  $1.50 \text{ \AA}$  indicate that the smectites are dioctahedral clay minerals with a revealed layer charge predominantly from octahedral sheets of montmorillonite. Other clay minerals are represented by mica

(illite, muscovite) with a basal reflection series of  $d \approx 10.0, 4.99, \text{ and } 3.34 \text{ \AA}$  and kaolinite with  $d(001) \approx 7.24 \text{ \AA}$  and other nonbasal reflections overlap with those of montmorillonite. The nonclay minerals were identified as feldspar (microcline) at  $d \approx 6.48, 4.03, 3.21, \text{ and } 3.18 \text{ \AA}$  and as quartz ( $d \approx 4.26, 3.34, 2.45, 2.38, 1.82, 1.52 \text{ \AA}$ , based on the JCPDS International Center for Diffraction Data). Quantitative calculations based on XRD data of randomly oriented specimens (Fig. 1a) indicated a rise from 40 wt.% of smectite content in untreated Di Linh bentonite to 61–63 wt.% in treated clays (Table 1) a considerable reduction in kaolinite content after modification was observed.

Concerning the oriented mounts, the full expandability of  $d(001)$  after ethylene glycol saturation confirmed the smectite phase's dominance before and after modification. The profile shapes of the  $d(001)$  reflections of the air-dried samples are asymmetric, which indicates the presence of two possible montmorillonite, mixed-layer phases with different interlayer cations in the interlayer sheet of montmorillonite (Fig. 1).

The FT-IR spectrum confirmed Al-smectite as the dominant phase in the samples (Fig. 2). The untreated Di Linh bentonite exhibits bands at  $469 \text{ cm}^{-1}$  (Si-O-Si deformation),  $532 \text{ cm}^{-1}$  (Al-O-Si deformation),  $1043 \text{ cm}^{-1}$  (Si-O stretching),  $3620 \text{ cm}^{-1}$  (stretching) and a small band at  $834 \text{ cm}^{-1}$  (Al-OH-Mg deformation). A shoulder at  $873 \text{ cm}^{-1}$  (Al-OH- $\text{Fe}^{3+}$  deformation) and a band at  $910 \text{ cm}^{-1}$  (Al-OH-Al deformation) corresponds to the substitution of Al for  $\text{Fe}^{3+}$  in the octahedral sheet of montmorillonite as well as the dominance of Al in this layer. The molecular water of montmorillonite is characterized by a band at  $1630 \text{ cm}^{-1}$  (not shown) and  $3420 \text{ cm}^{-1}$  (OH stretching region). In addition, diagnostic bands of kaolinite were observed at  $3699 \text{ cm}^{-1}$ , a band with lower intensities. Double bands identified the presence of quartz at  $796 \text{ cm}^{-1}$  and  $778 \text{ cm}^{-1}$ .

Table 1. Mineralogical compositions (bulk sample) and technique parameters of natural and Al-modified Di Linh bentonite

| Samples (wt.%)          | Di Linh* | C 1.2 | C 1.3 | C 1.4 | C 1.5 | C 1.6 | C 1.7 |
|-------------------------|----------|-------|-------|-------|-------|-------|-------|
| Mineral compositions    |          |       |       |       |       |       |       |
| Smectite                | 40       | 63    | 62    | 62    | 63    | 62    | 61    |
| Illite                  | 2        | <1    | 5     | 4     | 4     | 3     | 3     |
| Kaolinite               | 41       | 10    | 8     | 6     | 5     | 7     | 11    |
| Chlorite                | -        | -     | 3     | 5     | 3     | 6     | 5     |
| Muscovite               | 5        | 8     | 8     | 9     | 9     | 9     | 9     |
| Quartz                  | 10       | 16    | 13    | 15    | 15    | 15    | 13    |
| Microcline              | <1       | 3     | 4     | 5     | 4     | 6     | 5     |
| Calcite                 | -        | -     | <1    | <1    | <1    | <1    | <1    |
| Gypsum                  | -        | -     | <1    | <1    | <1    | <1    | <1    |
| Goethite                | <1       | <1    | <1    | <1    | <1    | <1    | <1    |
| Hematite                | -        | <1    | <1    | <1    | <1    | <1    | <1    |
| Rutile                  | <1       | <1    | <1    | -     | <1    | <1    | <1    |
| Technique parameters    |          |       |       |       |       |       |       |
| BET (m <sup>2</sup> /g) | 68.0     | -     | -     | 15.4  | -     | 15.0  | -     |
| Pore volume (cc/g)      | 0.102    | -     | -     | 0.103 | -     | 0.088 | -     |
| Pore diameter (Å)       | 39.44    | -     | -     | 35.45 | -     | 33.61 | -     |
| Pore size (Å)           | 67.5     | -     | -     | 32.4  | -     | 29.9  | -     |
| CEC (100 meq/100 g)     | 45       | 45    | -     | 88    | -     | 82    | -     |

Note: \* Mineral composition data were obtained from Hoang-Minh et al. (2019)

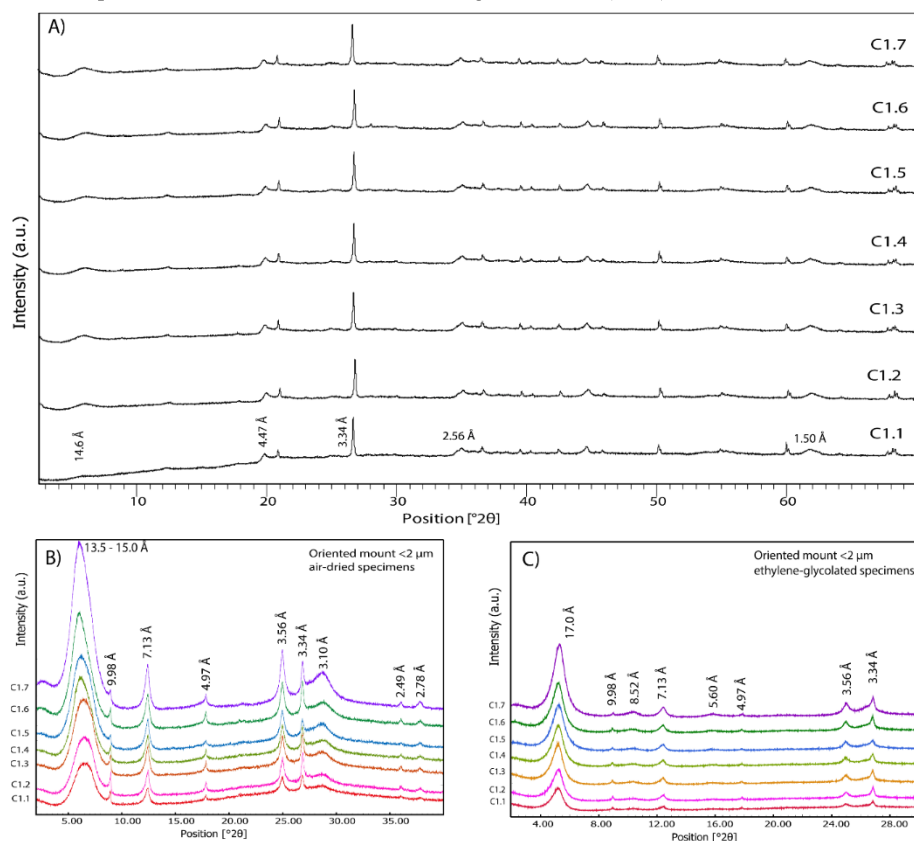


Figure 1. Diffraction diagrams of a) randomly oriented specimens, b) air-dried oriented mounts, and c) ethylene-glycol oriented mounts of Di Linh bentonites

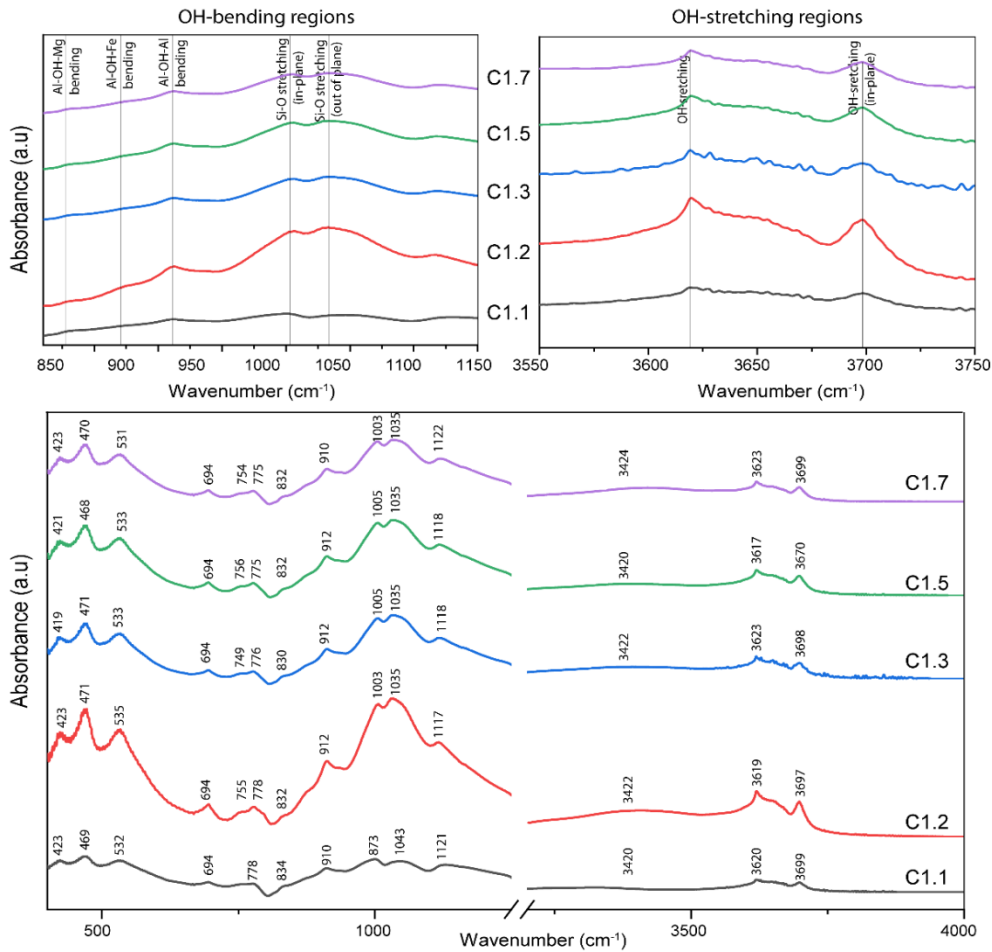


Figure 2. FT-IR spectra of representative samples of natural (C1.1) and Al-modified (C1.2, C1.3, C1.5, C1.7) Di Linh bentonites

Among the samples, the treated bentonites show increased intensities of the deformation vibrations of the Al-OH-Al bands in the octahedral sheets. In contrast, the intensities of the Al-OH-Mg and Al-OH-Fe bands remain unchanged. The increasing absorbance of the Si-O-Si band in the range of 1100–1050  $\text{cm}^{-1}$  and displacement of the band from 1043  $\text{cm}^{-1}$  to 1035  $\text{cm}^{-1}$  indicate a higher number of Si-O-Si bonds in the Al-modified bentonites. The increased intensities of the adsorption bands characteristic of amorphous silica at 1112–1118  $\text{cm}^{-1}$  and the enhanced intensity of the 471  $\text{cm}^{-1}$  band suggest a higher amount of amorphous silica after Al modification. The

increase in adsorbed water bands in the FT-IR spectra within 2500–3600  $\text{cm}^{-1}$  (3422  $\text{cm}^{-1}$ ) of Al-modified samples indicated a decrease in crystallite size and/or domain size.

In conclusion, the clays were characterized by Al-smectite as the dominant phase. Differences were observed between untreated Di Linh bentonite and treated samples in smectite and non-smectite phases' quantity and structure.

### 3.2. Morphology and surface area characterization

SEM images reveal the morphological characteristics of smectite, displaying plate-

like structures with numerous aggregates (Fig. 3). Needle-like particles are commonly observed growing on the edges of xenomorphic and discrete plates. Among the samples, the morphology did not differ significantly; however, the average size of the clay particles and aggregates decreased in the Al-modified clays, with numerous erosion

traces observed on the edges and surfaces of the clay particles. This observation can be explained by structural transformation due to attack by the  $H_2SO_4$  acid solution. During Al activation, the edges of the smectite layer are opened and detached, and some of the original smectite layers remain unaffected in the center of the particle.

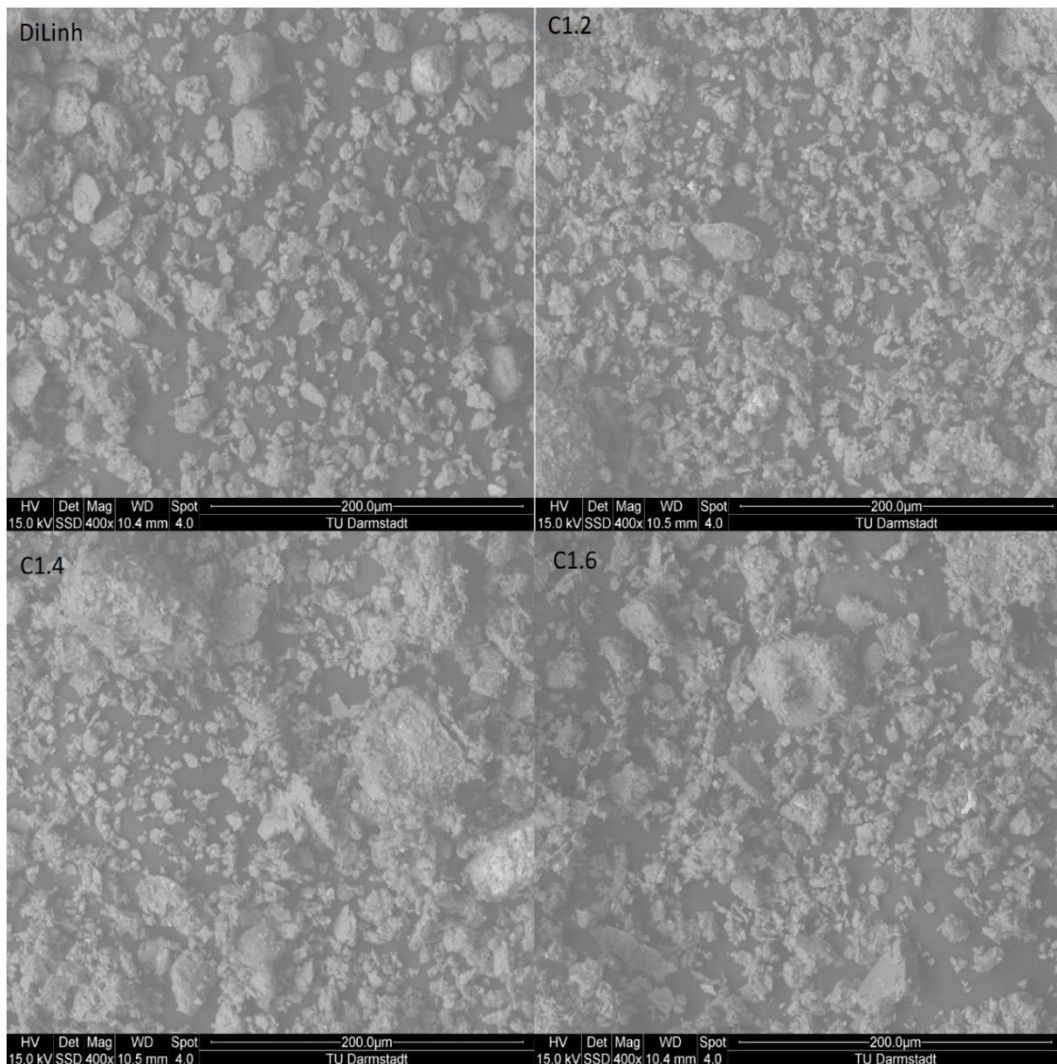


*Figure 3.* SEM images of representative samples of natural and Al-modified bentonites.  
*Note:* The brighter area presents bentonites; the darker area is the graphite-covered Cu-grid background

The typical behavior of smectite, exhibiting low nitrogen adsorption at low relative pressures in both natural and modified clays,

was confirmed by the  $N_2$  adsorption-desorption isotherm study (Fig. 4). The results indicated a minimal contribution to micropore capture

(<2 nm) but confirmed the presence of mesopores (2–50 nm). This characteristic aligns with the interparticle voids in clay minerals, as evidenced by increased adsorption in the mono-multilayer filling region. Otherwise, nitrogen adsorption continuously increased at higher relative pressures due to the enlargement of voids between aggregated particles, resulting in larger mesopores. A slight increase in nitrogen adsorption at low relative pressure was observed in the Al-modified clays (C1.4) compared to the untreated clays, indicating the presence of both micropores and mesopores, characteristic of type II physisorption isotherms (Thommes et al., 2015).

The hysteresis loops of the three selected samples also demonstrated the dominance of mesopores, which are classified as a mixture of H3-type and H4-type mesopores (IUPAC classifications, Thommes et al., 2015). This hysteresis loop corresponded to the interaction between nonrigid lamellar particles. It indicated an association of aggregates of plate-like particles, giving rise to slit-like pores (mesopores) (Cardoso et al., 2006).

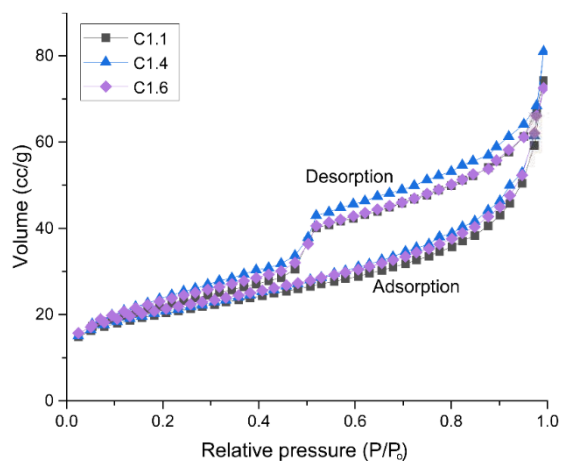


Figure 4. Adsorption isotherms of nitrogen on the natural (C1.1) and Al-modified (C1.4; C1.6) Di Linh bentonites

The average pore size in the untreated clay was 6.8 nm, and this parameter decreased to

approximately 3.2 (C1.4) and 3.0 nm (C1.6) after the experiment, while the total pore volume remained constant or decreased slightly at high concentrations of Al solution (Table 1). The clay's smaller grain size cannot explain these results but are likely related to the formation of porous structures due to the transformation of smectite after interaction with Al and H<sub>2</sub>SO<sub>4</sub>.

The measured BET-specific surface area decreased from 68 m<sup>2</sup>/g in the natural clay to 15 m<sup>2</sup>/g in the modified clays (Table 1) due to the Al modification process. This result was unexpected, as specific surface area values typically increase with higher smectite contents and CEC values (nearly doubled). There may be several reasons for this: (1) the formation of a minor distance in the interlayer sheet due to the substitution of divalent cations (Ca<sup>2+</sup> and Mg<sup>2+</sup>) for monovalent cations (Na<sup>+</sup>) in Al-modified clays and (2) the effect of Al (larger molecular size) from the Al solution (formation of hydroxy-interlayered Al), which results in the inaccessible nature of the internal surface to N<sub>2</sub> and the blocking of the pores in the Al-modified clay. The same results were observed previously by Seki and Yurdakoç (2005); Burns et al. (2006).

In sum, the materials' morphology remained unchanged after Al modification, but the particle size decreased, and erosion traces were observed on the edges, indicating structural transformation. The surface area analysis showed a significant decrease in BET values, which was unexpected given the increased smectite contents.

### 3.3. Effects of the Al-modified process

The results show that Di Linh bentonite's chemical compositions, structural properties, and morphological characteristics changed after Al modification. This could be due to the availability of Al and H<sub>2</sub>SO<sub>4</sub> acid as a result of



dilution between the  $\text{Al}_2(\text{SO}_4)_3 \cdot 18\text{H}_2\text{O}$  salt and water.

Changes in interlayer cations, as indicated by XRD results (shift in  $d(001)$ ), were also mentioned by Sapag and Mendioroz (2001). They stated that the interlayer cations are easily hydrolyzable, increasing the swelling potential and enlargement of the interlayer, which ultimately permits their exchange with other external cations. Therefore, the interlayer cations first substitute for each other cations, possibly forming an aluminum hydroxyl layer; subsequently, substitution occurs with higher contents of Al and Si in octahedral and tetrahedral sheets, respectively. Tomić et al. (2011) also mentioned that the contact with  $\text{H}_2\text{SO}_4$  acid also led to the disintegration of the 2:1 structure of smectite, but first, the interlayer sheet was affected.

Changes in both the Al and Si contents in the structure of Di Linh smectite, as observed via XRD (increase in intensities from  $d(001)$  and  $d(021)$ ), FT-IR (increase in intensities in the smectite bands) and a smaller grain size (SEM images), demonstrated slight structural transformation. These changes can be explained by the securitization of existing mixed-layer phases, kaolinite, and illite, which increase their stacking after Al modification. The new montmorillonite layers grew directly on the preexisting particles, partly dissolved at the edges but remaining stable at the center following the dissolution-precipitation mechanism. This process caused an increase in the crystallite thickness of the clay minerals (e.g., smectite), as represented by the larger  $c_0$ -axis of this phase after treatment (Table 1). This process promotes the sorption and other properties of bentonite after structural modification.

Li et al. (2024) also state that the substitution of octahedral and tetrahedral sheets between Al for Fe and Mg and Si for Al promotes a negative charge at the basal surface and a positive charge at the edge of

smectite and consequently supports different interactions between particles and particles, such as edge-to-face, face-to-face, and edge-to-edge interactions, due to charge attraction. This led to the smaller particles and aggregates, as observed in TEM images (Fig. 3), lower pore size (Table 1), and higher water bands in FT-IR spectra (Fig. 2). The minimal changes in the Al-OH-Mg and Al-OH-Fe bands in the FT-IR results (Fig. 2) suggest that little to no leaching of octahedral Fe or Mg occurred, while the Al content increased during the Al treatment. Zakusin et al. (2015) described in their study that Al treatment and acid attack can also cause a decrease in the interlayer charge because of substitution between octahedral and tetrahedral sheets; consequently, the clay particles and their aggregates will decrease in size and thickness. However, the modified Di Linh bentonites still show mesopores as the dominant structure. Other researchers also mentioned that the porosity of clay can be strongly affected by acid attacks at high temperatures but not at room temperature (Bayram et al., 2010; Krupskaya et al., 2017).

The dissolution of a part of the clay particles and/or micro clay particles during modification enhances the interlayer ordering by partially substituting cations in this layer. Otherwise, this shift can also be a result of Al entering from the Al solution and/or leaching from the octahedral sheet into the interlayer sheet; consequently, an Al hydroxy interlayer will be formed (Viennet et al., 2016), especially at a high concentration of Al solution, which causes a connection between aluminum and oxygen at the beginning and then continuous contact with  $\text{H}^+$  ions. Finally, the leaching of interlayer  $\text{Ca}^{2+}$  in smectite can act as a source of Ca during the formation of new calcite and gypsum, which are found as new traces in Al-modified bentonites (Table 1). Kaolinite with decreased contents (XRD, Table 1) could also be altered (Belver et al., 2002).

The increase in smectite contents (montmorillonite and mixed-layer minerals) and CEC values (Table 1, Fig. 1), as well as the substitution of divalent cations ( $\text{Ca}^{2+}$  and  $\text{Mg}^{2+}$ ) to monovalent cations ( $\text{Na}^+$ ) during the treatment, results in changes in the swelling potential. However, the BET surface area analysis showed a significant decrease. This reduction is likely due to pore blockage caused by hydroxy-interlayered Al formation and the substitution of divalent cations with monovalent cations, limiting nitrogen accessibility to the internal surfaces.

In this study, Al modification of Di Linh bentonite resulted in higher smectite content, increased CEC values, enhanced smectitization of the modified clays, and reduced clay particle size and noticeable erosion on the edges and surfaces of smectite particles. The interaction between smectite and  $\text{Al}_2(\text{SO}_4)_3 \cdot 2\text{H}_2\text{O}$  solution can lead to the leaching of interlayer cations; solution can lead to the leaching of interlayer cations, the substitution of Al and Si into the octahedral and tetrahedral sheets, changes in  $\text{Al}^{3+}$  coordination, and the protonation of OH groups. These findings demonstrate that Al treatment enhances the structural organization of smectite and modifies its mineralogical

properties, potentially improving its adsorption and surface characteristics.

### 3.4. Ammonium adsorption on natural and Al-modified bentonites

The ammonium removal capacity of natural and different Al-modified bentonites using low (50 mg/L) and high (1000 mg/L)  $\text{NH}_4\text{Cl}$  solution concentrations is shown in Fig. 5. Generally, untreated clay showed poorer adsorption capacities for ammonium. The removal capacity improved when the clay was modified with an Al solution. At a lower ammonium concentration, the removal capacity of natural bentonite increased from 0.32 mg/g (15.8%) to 0.47 mg/g (23.3%) for the Al-modified bentonite at the highest Al-solution concentration (500 ppm). Otherwise, at a higher ammonium concentration, the removal capacity of ammonium continuously increased with increasing Al concentration from 17.2 mg/g (43%) for natural clay to 19.3 mg/g (48%) for the 250 ppm Al solution, then decreased at the higher Al concentration loading. Generally, the removal capacity of ammonium increased with increasing Al concentration. However, this upward trend began to decline at higher ammonium concentrations (1000 mg/L) and Al solution loadings (500 ppm  $\text{Al}_2(\text{SO}_4)_3 \cdot 18\text{H}_2\text{O}$ ).

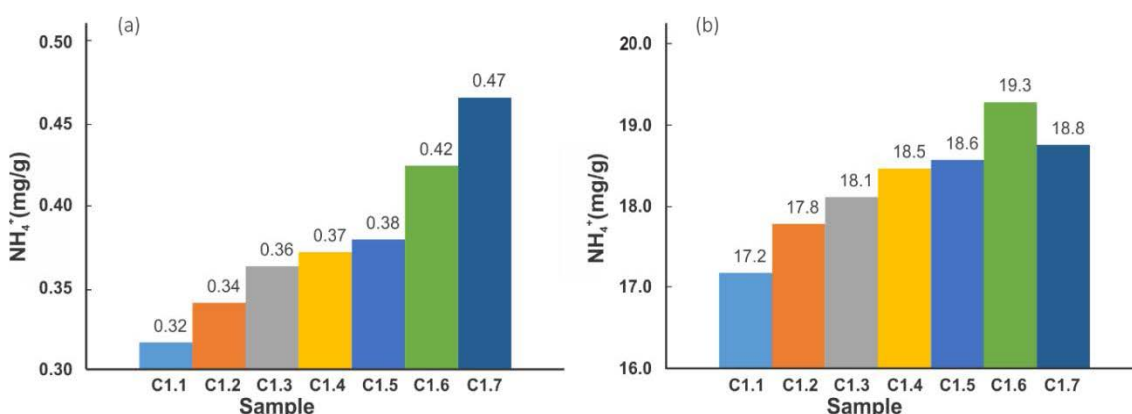


Figure 5. Comparison of ammonium removal efficiency in natural and Al-modified Di Linh bentonite at  $\text{NH}_4\text{Cl}$  concentrations of a) 50 mg/L and b) 1000 mg/L

This lower ammonium removal efficiency combined with the slower rate observed with the Al-modified materials is likely due to the competitive effect among divalent cations (e.g.,  $\text{Ca}^{2+}$ ,  $\text{Mg}^{2+}$ , and  $\text{Fe}^{2+}$ ) and monovalent cations ( $\text{Na}^+$  and  $\text{NH}_4^+$ ), which are leached from the clay structure to the solution. Ultimately, Al-smectite (montmorillonite) prefers affinity toward divalent cations when none of these ions are present at extremely high concentrations. Consequently, modifying clay with an Al solution facilitates the exchange of surfactant molecules, which attach to the surface of modified clay particles.

This surfactant's enhanced removal capacity of ammonium is attributed to alterations in the surface properties of the clay hybrids throughout the treatment process. Ultimately, these surfactant cations attract and electrostatically bind with ammonium ions. Moreover, the modification process also caused more surfactant molecules to form on

the site of the particles and strengthened the attachment of  $\text{Al}^{3+}$  and  $\text{SO}_4^{2-}$  on the surface of the smectite. A change in the surface and edges of smectite particles during modification promotes attachment and improves electrostatic contact with anionic surfactant cations. Tomić et al. (2011) stated the higher the acid concentration was, the greater the specific surface area because of increased porosity and decreased particle size. This result can be explained by the higher absorption capacity and higher  $\text{Al}_2(\text{SO}_4)_3 \cdot 18\text{H}_2\text{O}$  loading.

Table 2 compares the equilibrium adsorption capacities of untreated and Al-modified Di Linh bentonites with those of other bentonites used for  $\text{NH}_4^+$  removal in aqueous solutions. The results indicate that Di Linh bentonites demonstrate a significantly higher adsorption capacity than others, highlighting their potential as effective adsorbents for  $\text{NH}_4^+$  removal from water.

Table 2. Comparison of the adsorption capacity of raw and Al-modified Di Linh bentonites with other adsorbents

| Adsorbent                      | $\text{NH}_4^+$ -N Concentration (mg/L) | Adsorption capacity (mg/g) | Reference               |
|--------------------------------|---|----------------------------|-------------------------|
| Raw Di Linh bentonite          | 50                                      | 0.32                       | This study              |
| Al-modified Di Linh bentonite  | 50                                      | 0.47                       | This study              |
| Raw Di Linh bentonite          | 1000                                    | 17.2                       | This study              |
| Al-modified Di Linh bentonite  | 1000                                    | 19.3                       | This study              |
| Bentonite from Algeria         | 1000                                    | 46.85                      | Angar et al., 2017      |
| Ca-bentonite from Turkey       | 1000                                    | 0.50                       | Şahin et al., 2018      |
| Natural zeolite from Australia | 1000                                    | 8.2                        | Wijesinghe et al., 2016 |
| Treated zeolite from Australia | 1000                                    | 11.0                       | Wijesinghe et al., 2016 |

In general, the specific surface area of clay has a limited impact on the removal capacity of smectite. Still, this transformation significantly changes the smectite content, CEC, interlayer, and edge charge. It is the most critical factor in promoting the sorptive capacity of ammonium in Di Linh smectite.

#### 4. Conclusions

This study characterized Di Linh bentonite's mineralogical composition, structure, and properties and its ability to be

modified to be used as a sorbent for ammonium ions. The Al modification process was proven by the increase in smectite phases and substitution in the interlayer, octahedral layer, and tetrahedral layer that led to the chemical and physical transformation of clay particles, as observed by XRD, FT-IR, and SEM data. The  $\text{H}_2\text{SO}_4$  acid during the dilution of  $\text{Al}_2(\text{SO}_4)_3 \cdot 18\text{H}_2\text{O}$  strongly affects this transformation process. Otherwise, the lower specific surface area and mostly unchanged development of microporous structures were

found in the BET and N<sub>2</sub> adsorption-desorption results. Thus, the BET surface area and microporous structure are not significant factors influencing the absorptive properties of ammonium.

The adsorption capacity of ammonium in Al-modified bentonites is more significant than that in natural bentonite at both low and high ammonium concentrations. The study showed the strong influence of the Al-solution concentration on the absorption capacity of ammonium from clays. Otherwise, at higher concentrations, the sorptive capacity is more significant. These characteristics are likely related to the combination of two transformation factors of clay: (1) the formation of smaller but thicker clay particles related to smectitization with more smectite in Al-modified bentonites and (2) the increase in electrostatic interactions between the surface and edge of particles with Al<sup>3+</sup> and SO<sub>4</sub><sup>2-</sup> in solution.

Because Al-modification causes slight mineralogical transformation and can add a small microporous structure and a lower specific surface area, the smectitic layers could be weakly acidic to attract ammonium. Therefore, Al-modified Di Linh bentonites increased ammonium adsorption compared to natural Di Linh bentonite.

### Acknowledgments

The authors thank the Institute of Geosciences at Goethe University Frankfurt and the Institute of Material Sciences at the Technical University Darmstadt for their assistance with specific analyses. This study was funded by the Vietnam National Foundation for Science and Technology Development (NAFOSTED) (grant number 105.99-2019.311).

### References

Abu Hasan H., Sheikh Abdullah S.R., Kamarudin S.K., Tan Kofli N., 2013. On off control of aeration time

- in the simultaneous removal of ammonia and manganese using a biological aerated filter system. *Process Saf Environ*, 91(5), 415–422. <https://doi.org/10.1016/j.psep.2012.10.001>.
- Angar Y., Djelali N.E., Kebbouche-Gana S., 2017. Investigation of ammonium adsorption on Algerian natural bentonite. *Environ Sci Pollut Res Int*, 24, 11078–11089. <https://doi.org/10.1007/s11356-016-6500-0>.
- Anggraini M., Kurniawan A., Ong L.K., Martin M.A., Liu J.C., Soetaredjo F.E., Indraswati N., Ismadji S., 2014. Antibiotic detoxification from synthetic and real effluents using a novel MTAB surfactant montmorillonite (organoclay) sorbent. *RSC Adv*, 4, 16298–16311. <https://doi.org/10.1039/C4RA00328D>.
- Bayram H., Önal M., Yılmaz H., 2010. Thermal analysis of a white calcium bentonite. *J. Therm Anal Calorim*, 101, 873–879. <https://doi.org/10.1007/s10973-009-0626-y>.
- Bhattacharyya K.G., Gupta S.S., 2008. Adsorption of a few heavy metals on natural and modified kaolinite and montmorillonite: A review. *Adv Colloid Interface Sci.*, 140(2), 114–131. <https://doi.org/10.1016/j.cis.2007.12.008>.
- Burns S.E., Bartelt-Hunt S.L., Smith J.A., Redding A.Z., 2006. Coupled mechanical and chemical behavior of bentonite engineered with a controlled organic phase. *J Geotech Geoenviron Eng.*, 132(11), 1404–1412. [https://doi.org/10.1061/\(ASCE\)1090-0241\(2006\)132:11\(1404\)](https://doi.org/10.1061/(ASCE)1090-0241(2006)132:11(1404)).
- Campos J.C., Moura D., Costa A.P., Yokoyama L., Araujo F.V.F., Cammarota M.C., Cardillo L., 2013. Evaluation of pH, alkalinity and temperature during air stripping process for ammonia removal from landfill leachate. *J Environ Sci Health A Tox Hazard Subst Environ Eng*, 48(9), 1105–1113. <https://doi.org/10.1080/10934529.2013.774658>.
- Cardoso P.L., Celis R., Cornejo J., Valim J.B., 2006. Layered double hydroxide as supports for the slow release of acid herbicides. *J Agric Food Chem*, 54, 5968–5975.
- Chai L., Peng C., Min X., Tang C., Song Y., Zhang Y., Zhang J., Ali M., 2017. Two-sectional struvite formation process for enhanced treatment of copper-

- ammonia complex wastewater. *Trans Nonferrous Met Soc China*, 27(2), 457–466. [https://doi.org/10.1016/S1003-6326\(17\)60052-9](https://doi.org/10.1016/S1003-6326(17)60052-9).
- Cheng H., Zhu Q., Xing Z., 2019. Adsorption of ammonia nitrogen in low temperature domestic wastewater by modification bentonite. *J. Clean Prod*, 233, 720–730. <https://doi.org/10.1016/j.jclepro.2019.06.079>.
- Dontsova K.M., Norton L.D., Johnson C.T., 2005. Calcium and magnesium effect on ammonia adsorption by soil clays. *Soil Sci Soc Am J.*, 69, 1225–1232. <https://doi.org/10.2136/sssaj2004.0335>.
- dos Santos P.R., Daniel L.A., 2020. A review: organic matter and ammonia removal by biological activated carbon filtration for water and wastewater treatment. *Int J Environ Sci Technol*, 17, 591–606.
- Ducey T.F., Vanotti M.B., Shriner A.D., Szogi A.A., Ellison A.Q., 2010. Characterization of a microbial community capable of nitrification at cold temperature. *Bioresour Technol*, 101(2), 491–500. <https://doi.org/10.1016/j.biortech.2009.07.091>.
- Dukic A.B., Kumric K.R., Vukelic N.S., Dimitrijevic M.S., Bascarevic Z.D., Kurko S.V., Matovic L.L., 2015. Simultaneous removal of  $Pb^{2+}$ ,  $Cu^{2+}$ ,  $Zn^{2+}$  and  $Cd^{2+}$  from highly acidic solutions using mechanochemically synthesized montmorillonite-kaolinite/ $TiO_2$  composite. *Appl Clay Sci.*, 103, 20–27. <https://doi.org/10.1016/j.clay.2014.10.021>.
- Edwards T.M., Puglis H.J., Kent D.B., Duran J.L., Bradshaw L.M., Farag A.M., 2024. Ammonia and aquatic ecosystems - a review of global sources, biogeochemical cycling, and effects on fish. *Sci Total Environ*, 907, 167911. <https://doi.org/10.1016/j.scitoenv.2023.167911>.
- Farmer V.C., 1974. *The Infrared Spectra of Minerals*, Monograph, fourth ed. Mineralogical Society, London.
- Han B., Butterly C., Zhang W., He J.-Z., Chen D., 2021. Adsorbent materials for ammonium and ammonia removal: a review. *J Clean Prod*, 283, 124611. <https://doi.org/10.1016/j.jclepro.2020.124611>.
- Hoang-Minh T., Kasbohm J., Nguyen-Thanh L., Nga P.T., Lai L.T., Duong N.T., Thanh N.D., Thuyet N.T.M., Anh D.D., Pusch R., Knutsson S., Ferreira Mählmann R., 2019. Use of TEM-EDX for structural formula identification of clay minerals: a case study of Di Linh bentonite, Vietnam. *J Appl Cryst*, 52, 133–147. <https://doi.org/10.1107/S1600576718018162>.
- Ianchis R., Rosca I.D., Ghiurea M., Spataru C.I., Nicolae C.A., Gabor R., Raditoiu V., Preda S., Fierascu R.C., Donescu D., 2015. Synthesis and properties of new epoxy-organolayered silicate nanocomposites. *Appl Clay Sci.*, 103, 28–33. <https://doi.org/10.1016/j.clay.2014.10.020>.
- Ji Y., Bai J., Li J., Luo T., Qiao L., Zeng Q., Zhou B., 2017. Highly selective transformation of ammonia nitrogen to  $N_2$  based on a novel solar-driven photoelectrocatalytic-chlorine radical reactions system. *Water Res*, 125, 512–519. <https://doi.org/10.1016/j.watres.2017.08.053>.
- Jorgensen T.C., Weatherley L.R., 2003. Ammonia removal from wastewater by ion exchange in the presence of organic contaminants. *Water Res*, 37(8), 1723–1728. [https://doi.org/10.1016/S0043-1354\(02\)00571-7](https://doi.org/10.1016/S0043-1354(02)00571-7).
- Krupskaya V.V., Zakusin S.V., Tyupina E.A., Dorzhieva O.V., Zhukhlistov A.P., Belousov P.E., Timofeeva M.N., 2017. Experimental Study of Montmorillonite structure and transformation of its properties under treatment with inorganic acid solutions. *Minerals*, 7, 49. <https://doi.org/10.3390/min7040049>.
- Kurniawan A., Sutiono H., Ju Y.-H., Soetaredjo F.E., Ayucitra A., Yudha A., Ismadi S., 2011. Utilization of rarasaponin natural surfactant for organo-bentonite preparation: Application for methylene blue removal from aqueous effluent. *Microporous Mesoporous Mater*, 142(1), 184–193. <https://doi.org/10.1016/j.micromeso.2010.11.032>.
- Lagaly G., Ziesmer S., 2003. Colloid chemistry of clay minerals: the coagulation of montmorillonite dispersions. *Adv Colloid Interface Sci.*, 100–102, 105–128. [https://doi.org/10.1016/S0001-8686\(02\)00064-7](https://doi.org/10.1016/S0001-8686(02)00064-7).
- Li J., Ma H., Yan Y., Zhang J., Li Z., 2024. Molecular insights into the aggregation mechanism of montmorillonite colloid due to calcium contamination: A molecular dynamics simulation study. *Appl Clay Sci.*, 247, 107191. <https://doi.org/10.1016/j.clay.2023.107191>.
- Lin L., Lei Z., Wang L., Liu X., Zhang Y., Wan C., Lee D.-J., Tay J.H., 2013. Adsorption mechanisms of



- high-levels of ammonium onto natural and NaCl-modified zeolites. *Sep Purif Technol*, 103, 15–20. <https://doi.org/10.1016/j.seppur.2012.10.005>.
- Lin L., Wan C., Lee D.-J., Lei Z., Liu X., 2014. Ammonium assists orthophosphate removal from high-strength wastewaters by natural zeolite. *Sep Purif Technol*, 133, 351–356. <https://doi.org/10.1016/j.seppur.2012.10.005>.
- Lin S.H., Juang R.S., 2002. Heavy metal removal from water by sorption using surfactant-modified montmorillonite. *J Hazard Mater*, 92(3), 315–326. [https://doi.org/10.1016/S0304-3894\(02\)00026-2](https://doi.org/10.1016/S0304-3894(02)00026-2).
- Liu Y., Ngo H.H., Guo W., Peng L., Wang D., Ni B., 2019. The roles of free ammonia (FA) in biological wastewater treatment processes: a review. *Environ Int*, 123, 10–19. <https://doi.org/10.1016/j.envint.2018.11.039>.
- Madejová J., Komadel P., 2001. Baseline studies of The Clay Minerals Society Source Clays: Infrared methods. *Clays Clay Miner*, 49, 410–432. <https://doi.org/10.1346/CCMN.2001.0490508>.
- Murray H.H., 2007. Applied Clay Mineralogy: Occurrences, Processing and Application of Kaolins, Bentonites, Palygorskite-Sepiolite, and Common Clays. In H. H. Murray (Ed.). *Developments in Clay Science*. Elsevier, Amsterdam, 2, 180p.
- Pandey S., 2017. A comprehensive review on recent developments in bentonite-based materials used as adsorbents for wastewater treatment. *J Mol Liq*, 241, 1091–1113. <https://doi.org/10.1016/j.molliq.2017.06.115>.
- Rajeshwari K.V., Balakrishnan M., Kansal A., Lata K., Kishore V.V.N., 2000. State of-the-art of anaerobic digestion technology for industrial wastewater treatment. *Renew Sustain Energy Rev*, 4(2), 135–156. [https://doi.org/10.1016/S1364-0321\(99\)00014-3](https://doi.org/10.1016/S1364-0321(99)00014-3).
- Rybalkina O.A., Tsygurina K.A., Melnikova E.D., Pourcelly G., Nikonenko V.V., Pismenskaya N.D., 2019. Catalytic effect of ammonia-containing species on water splitting during electro dialysis with ionexchange membranes. *Electrochim Acta*, 299, 946–962.
- Rzayev Z.M.O., Uzgoren-Baran A., Bunyatova U., 2015. Functional organo-Mt/copolymer nanoarchitectures: microwave-assisted rapid synthesis and characterization of ODA-Mt/poly[NIPAm-co-(MA-alt-2,3-2H-DHP)] nanocomposites. *Appl Clay Sci*, 105–106, 1–13. <https://doi.org/10.1016/j.clay.2014.12.015>.
- Şahin D., Öz M., Sertasi E., Öz Ü., Karsli Z., Aral O., 2018. Evaluation of natural minerals (zeolite and bentonite) for nitrogen compounds adsorption in different water temperatures suitable for aquaculture. *Int Lett Nat Sci*, 71, 34–42. <https://doi.org/10.18052/www.scipress.com/ILNS.71.34>.
- Sapag K., Mendioroz S., 2001. Synthesis and characterization of micromesoporous solids: pillared clays. *Colloids Surf A: Physicochem Eng Asp*, 187–188, 141–149. [https://doi.org/10.1016/S0927-7757\(01\)00617-3](https://doi.org/10.1016/S0927-7757(01)00617-3).
- Seki Y., Yurdakoç K., 2005. Paraquat adsorption onto clays and organoclays from aqueous solution. *J Colloid Interface Sci*, 287(1), 1–5. <https://doi.org/10.1016/j.jcis.2004.10.072>.
- Sing K.S.W., Everett D.H., Haul R.A.W., Moscou L., Pierotti R.A., Rouquerol J., Siemieniewska T., 1984. Reporting physisorption data for gas/solid systems with special reference to the determination of surface area and porosity. *Pure Appl Chem*, 57, 603–619. <https://doi.org/10.1351/pac198557040603>.
- Sotoft L.F., Pryds M.B., Nielsen A.K., Norddahl B., 2015. Process simulation of ammonia recovery from biogas digestate by air stripping with reduced chemical consumption. In: Gernaey KV, Huusom JK, Gani R (Eds.) *Computer Aided Chemical Engineering*. Elsevier, 2465–2470.
- Srinivasan R., 2011. Advances in application of natural clay and its composites in removal of biological, organic, and inorganic contaminants from drinking water. *Adv Mater Sci Eng*, 872531. <https://doi.org/10.1155/2011/872531>.
- Storek S., Bretinger H., Maier W.F. 1998. Characterization of micro- and mesoporous solids by physisorption methods and pore-size analysis. *Appl Catal A: General*, 174, 137–146. [https://doi.org/10.1016/S0926-860X\(98\)00164-1](https://doi.org/10.1016/S0926-860X(98)00164-1).
- Sun Z.M., Qu X.S., Wang G.F., Zheng S.L., Frost R.L., 2015. Removal characteristics of ammonium nitrogen from wastewater by modified Ca-bentonites. *Appl Clay Sci.*, 107, 46–51. <https://doi.org/10.1016/j.clay.2015.02.003>.

- Thommes M., Kaneko K., Neimark V.A., Oliver P.A., Rodriguez-Reinoso F., Rouquerol J., Sing S.W., 2015. Physisorption of gases, with special reference to the evaluation of surface area and pore size distribution (IUPAC Technical report). *Pure Appl Chem*, 87(9–10), 1051–1069. <https://doi.org/10.1515/pac-2014-1117>.
- Tomić Z.P., Antić Mladenović S.B., Babić B.M., Poharc Logar V.A., Djordjević A.R., Cupać S.B., 2011. Modification of smectite structure by sulfuric acid and characteristics of the modified smectite. *J Agric Sci*, 56, 25–35. <https://doi.org/10.2298/JAS1101025T>.
- Tran D.T., Pham T.D., Dang V.C., Pham T.D., Nguyen M., Dang N.M., Ha M.N., Nguyen V.N., Nghiem L.D., 2022. A facile technique to prepare MgO-biochar nanocomposites for cationic and anionic nutrient removal. *J Water Process Eng*, 47, 102702. <https://doi.org/10.1016/j.jwpe.2022.102702>.
- Tu Y., Feng P., Ren Y., Cao Z., Wang R., Xu Z., 2019. Adsorption of ammonia nitrogen on lignite and its influence on coal water slurry preparation. *Fuel*, 238, 34–43. <https://doi.org/10.1016/j.fuel.2018.10.085>.
- Vanamudan A., Pamidimukkala P., 2015. Chitosan, nanoclay and chitosan–nanoclay composite as adsorbents for Rhodamine-6G and the resulting optical properties. *Int J Biol Macromol*, 74, 127–135. <https://doi.org/10.1016/j.ijbiomac.2014.11.009>.
- Viennet J., Hubert F., Tertre E., Ferrage E., Robin V., Dzene L., Cochet C., Turpault M., 2016. Science direct effect of particle size on the experimental dissolution and autoaluminization processes of K-vermiculite. *Geochim Cosmochim Acta*, 180, 164–176. <https://doi.org/10.1016/j.gca.2016.02.005>.
- WHO (World Health Organization), 2011. Guidelines for drinking water quality (Fourth ed.). World Health Organization, Geneva.
- Wijesinghe D.T.N., Dassanayake K.B., Sommer S.G., Jayasinghe G.Y., Scales P.J., Chen D., 2016. Ammonium removal from high-strength aqueous solutions by Australian zeolite. *J Environ Sci Health A*, 51(8), 614–625. Doi: 10.1080/10934529.2016.1159861.
- Yang H., Li D., Zeng H., Zhang J., 2019. Impact of Mn and ammonia on nitrogen conversion in biofilter coupling nitrification and ANAMMOX that simultaneously removes Fe, Mn and ammonia. *Sci Total Environ*, 648, 955–961. <https://doi.org/10.1016/j.scitotenv.2018.08.223>.
- Zamparas M., Drosos M., Georgiou Y., Deligiannakis Y., Zacharias I., 2013. A novel bentonite-humic acid composite material Bephos™ for removal of phosphate and ammonium from eutrophic waters. *Chem Eng J*, 225, 43–51. <https://doi.org/10.1016/j.cej.2013.03.064>.
- Zheng H., Han L., Ma H., Zheng Y., Zhang H., Liu D., Liang S., 2008. Adsorption characteristics of ammonium ion by zeolite 13X. *J Hazard Mater*, 158(2), 577–584. <https://doi.org/10.1016/j.jhazmat.2008.01.115>.
- Zhou C.H., Zhang D., Tong D.S., Wu L.M., Yu W.H., Ismadji S., 2012. Paper-like composites of cellulose acetate–organo-montmorillonite for removal of hazardous anionic dye in water. *Chem Eng J*, 209, 223–234. <https://doi.org/10.1016/j.cej.2012.07.107>.